JOURNAL OF GEOPHYSICAL RESEARCH, VOL. 115, C07013, doi:10.1029/2009JC005884, 2010

Importance of heat transport and local air-sea heat fluxes for Barents Sea climate variability

A. B. Sandø,[1,2] J. E. Ø. Nilsen,[2,3] Y. Gao,[2,3,4] and K. Lohmann[5]

Received 8 October 2009; revised 15 March 2010; accepted 25 March 2010; published 22 July 2010.

[1] An isopycnic coordinate ocean model has been used to investigate the importance of different mechanisms on the Barents Sea climate variability for the period 1948–2006 Observed and simulated time series from the Kola Section are used to evaluate the model, and the model captures both the temperature and its variability. Based on lagged correlations between different climatological time series, it is shown here that heat transport through the Barents Sea Opening and solar heat flux are about equally important to the climate variability in the Barents Sea. The heat transport has greater potential of predictability due to a relatively long time lag. Furthermore, the non-solar and the net heat flux variability is governed by fluctuations in the oceanic heat content. All time series considered important for the Barents Sea climate variability show significant correlation to the North Atlantic Oscillation (NAO) pattern on a decadal time scale. As the associated low pressure system in the Nordic Seas moves eastward from 1948–1977 to 1978–2006, the correlation between NAO and heat transports into the Barents Sea becomes higher.

Citation: Sandø, A. B., J. E. Ø. Nilsen, Y. Gao, and K. Lohmann (2010), Importance of heat transport and local air-sea heat fluxes for Barents Sea climate variability, *J. Geophys. Res.*, *115*, C07013, doi:10.1029/2009JC005884.

1. Introduction

[2] The inflow of warm and saline Atlantic water into the Barents Sea and the ocean-atmosphere fluxes therein are of significant importance to the regional ocean climate, as well as for the biomass production and fish distribution within the Barents Sea [*Drinkwater et al.*, 2009; *Sakshaug et al.*, 1994]. It is therefore of particular interest to study their relative importance and the mechanisms behind the variability of the respective processes.

[3] The major inflow of waters to the Barents Sea occurs between Fugløya and Bear Island, called the Barents Sea Opening (BSO) (Figure 1). Moored current meters in the BSO [*Ingvaldsen et al.*, 2002, 2004; *Skagseth et al.*, 2008] have been used to estimate the inflow to the Barents Sea. The gap between the amount of observed hydrography and velocity data, and the resolution in time and space needed to investigate the mechanisms behind the long and short-term variability, is too large. Our approach is therefore to apply an Ocean General Circulation Model (OGCM), which provides simulated hydrography and current data with relatively good coverage for large ocean domains and periods of several decades. The model systems in general have undergone significant improvements over the last decades, and present OGCMs can often complement available ocean observations, and more importantly, be used as laboratories for assessing cause-effect relationships in the observed changes in the marine climate system [e.g., *Drange et al.*, 2005].

[4] The particular model system used for this study is presented in Section 2. In Section 3 we provide a brief description of the various analysis techniques used in this study, and results are shown in Section 4. The implications of the various findings are discussed in Section 5, before the paper is summarized and concluded in Section 6.

2. Model Description

[5] A modified version of the Miami Isopycnal Coordinate Ocean Model (MICOM) [*Bleck et al.*, 1992] has been used in this study of the Barents Sea. The horizontal resolution is about 40 km in the Barents Sea area. Vertically, a mixed layer model and 34 isopycnic layers are used with potential densities ranging from $\sigma = 21.22$ to $\sigma = 28.70$. The grid configuration is a global, non-eddy permitting one with focus in the North Atlantic region, achieved by locating the two poles of the grid over North America and the Caspian Sea.

[6] In isopycnic coordinate models the density is used as a vertical coordinate. The main reason for this kind of vertical discretization is that most of the transport in the ocean is believed to occur along isopycnal surfaces. The cross-isopycnal mixing in the ocean interior is order of magnitudes lower than the along-isopycnal mixing, and can in many model experiments be neglected [*Ledwell et al.*, 1993]. All numerical ocean models use advection schemes that contain

[1]Institute of Marine Research, Bergen, Norway.
[2]Bjerknes Centre for Climate Research, Bergen, Norway.
[3]Nansen Environmental and Remote Sensing Center, Bergen, Norway.
[4]Nansen-Zhu International Research Centre, Beijing, China.
[5]Max Planck Institute for Meteorology, Hamburg, Germany.

0148-0227/10/2009JC005884

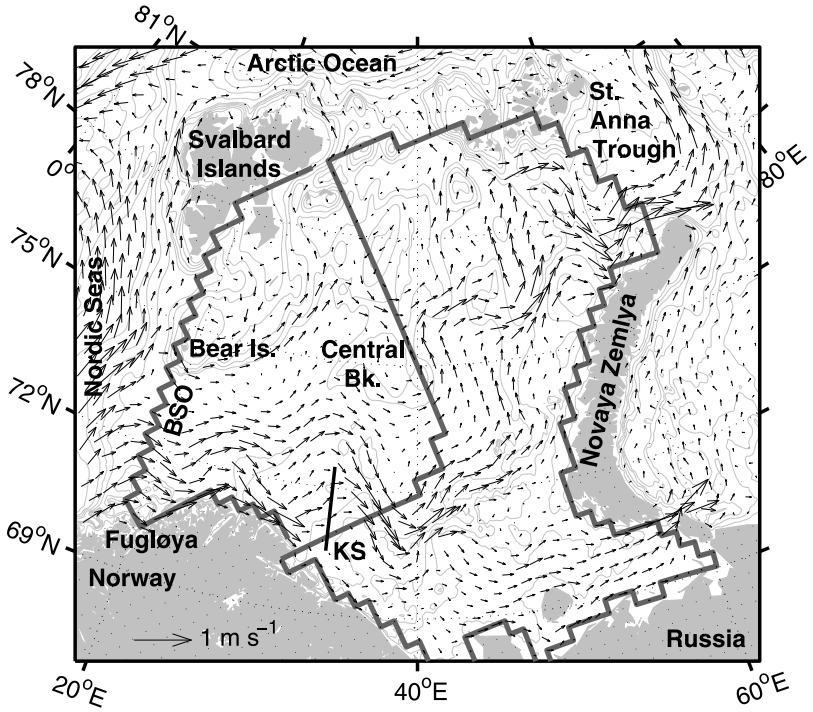

Figure 1. Map of the Barents Sea. Arrows indicate modeled mean flow in the upper 100 m of the ocean. Thick closed line defines the grid points of the eastern region, while thick open line defines the outside borders of the western region. The Kola Section (KS) is marked with straight black line. Isobaths for every 50 m are shown in grey.

numerical diffusion or mixing. In an isopycnic model, this artificial mixing will be directed along density surfaces, while ocean models using any other formulation in the vertical will introduce artificial diapycnal mixing whenever there are sloping isopycnals in the ocean which intersect the model coordinate surfaces. The isopycnic models therefore provide a means for studying these mixing processes without introducing false diapycnal mixing through the numerical scheme used, and thereby maintaining water masses with specific $T - S$ properties.

[7] This version includes several aspects that deviate from previous versions of MICOM. The most important modifications deal with the advection scheme, the choice of reference pressure, the pressure gradient force, and the diapycnal mixing. One major difference is that the model conserves heat and salt by the introduction of incremental remapping [*Dukowicz and Baumgardner*, 2000] as the transport algorithm. The remapping method also ensures that layer thicknesses and tracers are treated in a fully consistent way. In addition the model uses a more realistic parameterization of air–sea fluxes [*Bentsen and Drange*, 2000] and is therefore more suited to study effects of heat fluxes on the Barents Sea heat content.

[8] A dynamic and thermodynamic sea-ice model has been coupled to MICOM [*Bentsen*, 2002]. The models share the horizontal grid, the exchange of fluxes are handled internally, and the sea-ice model can therefore be considered as an integrated part of MICOM. The thermodynamic part of the sea-ice model is based on *Drange and Simonsen* [1996]. The dynamical part of the sea-ice model uses viscous-plastic rheology [*Hibler*, 1979] and is based on the implementation of *Harder* [1996].

[9] To avoid model drift in salinity, which inevitably influences the strength of the Atlantic meridional overturning circulation through the amount of salt being advected into the subpolar North Atlantic, a Newtonian relaxation of sea surface salinity is applied with a relaxation time scale of 30 days for a 50 m thick mixed layer, linearly decreasing with thicker mixed layers [see *Bentsen et al.*, 2004]. No relaxation was applied in waters where sea-ice is present in March in the Arctic and in September in the Antarctic to avoid relaxation towards salinity outliers in the poorly sampled polar waters. The mismatch between model and climatology were limited to 0.5 psu in the computation of the relaxation fluxes. Continental runoff is included by adding freshwater into the appropriate coastal grid cells [*Furevik et al.*, 2003].

[10] The atmospheric forcing used is taken from daily NCEP/NCAR reanalysis fields [*Kalnay et al.*, 1996], along with information of the sea surface state (temperature and sea ice concentration). The forcing scheme and procedure described by *Bentsen and Drange* [2000] is used here. The scheme reproduces the reanalysis fluxes if the model has the same surface state as in the reanalysis. These states will generally differ and then the fluxes are modified. The turbulent fluxes are modified consistently with the bulk parameterization of *Fairall et al.* [1996]. The *Berliand and Berliand* [1952] approach is used as a basis for the parameterization of the net long-wave radiation at the sea surface. For the net short-wave radiation, a function of incoming short-wave radiation and sea surface albedo is used, and the albedo is parameterized by the ocean model according to *Drange and Simonsen* [1996]. The turbulent fluxes of sensible and latent heat are based on the bulk expressions developed by *Smith et al.* [1996].

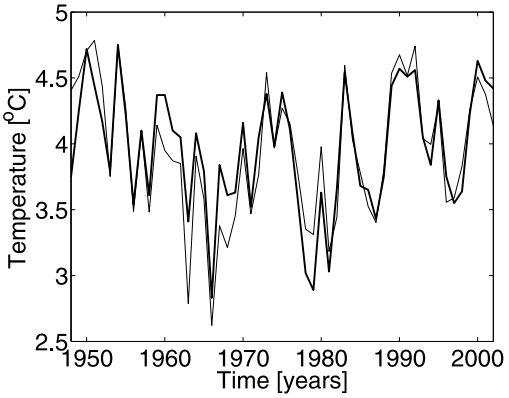

Figure 2. Time series of observed (thick) and simulated (thin) averaged temperatures in the Kola Section (upper 200 m). The time series are annual means.

[11] Model spin up is done using four consecutive cycles of daily reanalysis fields from 1948–2005, yielding a total spin-up period of more than 200 years. For the initial cycle, the hydrography is based on the January *Levitus et al.* [1994] and *Levitus and Boyer* [1994] climatological temperature and salinity fields, respectively, an ocean at rest, and a 2 m thick sea ice cover with extent according to climatology. For each subsequent spin up cycle, the initial ocean state is taken from the end state of the previous cycle.

[12] For a more detailed description of the model physics and the performance, we refer the reader to previous studies [*Nilsen et al.*, 2003; *Bentsen et al.*, 2004; *Gao et al.*, 2004; *Drange et al.*, 2005; *Hátun et al.*, 2005a, 2005b; *Eldevik et al.*, 2005; *Mauritzen et al.*, 2006; *Orre et al.*, 2007]. In general, the model system has demonstrated good skills in simulating the ocean circulation and thermodynamics in the Atlantic and Arctic waters.

3. Methods

[13] First, time series of observed and modeled temperatures from the Kola Section in the Barents Sea are compared to evaluate the model with respect to temperature in this area. Such an evaluation is useful and necessary in order to justify the use of model results in a cause-effect study like this. Thereafter, time series of modeled temperature, heat- and volume transports through the BSO, air–sea heat fluxes, and integrated heat content in the Barents Sea have been compared and correlated in order to find the controlling factors for the climate variability. The correlation and the corresponding sign may indicate a physical relation between the time series, while the lag between them may be an expression for a delay due to advection or dispersion of the physical quantities of interest. Sea level pressure has also been correlated and regressed against the time series to find the dominating atmospheric pattern linked to the variability, and to what degree it is important.

4. Results

4.1. Model Evaluation

[14] The Barents Sea is among the few ocean areas where long observational time series are available. The institute of marine research in Murmansk (PINRO) has since 1900 monitored temperature in the Kola Section, crossing the Atlantic water flow in the Barents Sea (along 33.5°E from 70.5°N to 72.5°N in 5 stations). Observations are taken on monthly basis [*Hughes et al.*, 2009] in the entire water column which depth varies from 150m to 350m. The Kola section corresponds to about 6 grid points in the model. The time series of observed and simulated annual mean temperature anomalies in Figure 2 shows long time variability with a cycle of several decades. The mean of the observed temperatures is 3.96°C, and simulated mean temperature is 3.94°C. The correlation between observed and simulated temperatures is $r = 0.89$, and it is evident that the model captures the observed temperature and its variability.

[15] The average modeled heat transport into the Barents Sea through the BSO is 74 TW. This concurs well with the available observational estimates of a total BSO heat transport of 73 TW [*Skagseth et al.*, 2008; *Gammelsrød et al.*, 2009; *Smedsrud et al.*, 2010; Ø. Skagseth et al., Wind-induced transport of the Norwegian Coastal Current in the Barents Sea, submitted to *Journal of Geophysical Research*, 2009], as well as the numerical simulation by *Harms et al.* [2005] also at 73 TW. For the St. Anna Trough, the main outflow in both model and reality, the comparison is also reasonable (model: 1.95 Sv and −11 TW; observations: 1.8 Sv and −3.6 TW [*Gammelsrød et al.*, 2009]) especially given the large uncertainties of estimates from this extremely scarcely sampled opening.

4.2. Heat Content, Heat Transports, and Heat Fluxes

[16] The Barents Sea climate variability is in this study described in terms of time series of heat content integrated in the whole model ocean volume (both boxes, Figure 1). This heat content is mainly determined by the heat transport through the BSO (net 74 TW; standard deviation 20 TW) and the heat fluxes to the atmosphere (net 94 TW; standard deviation 42 TW). The heat transports through the St. Anna Trough, has an order of magnitude weaker variability (standard deviation 4 TW), and the contribution from outflow variability will be neglected accordingly.

[17] Figures 3 and 4 show normalized time series of simulated annual heat content together with heat transport and heat flux, respectively, all computed from monthly time series.

[18] The similarity between curves shows that the heat content follows the BSO heat transports during the entire period. Also the heat content and the heat fluxes show similar variability, especially on longer time scales.

[19] The question is how the two main heat input and output mechanisms govern the Barents Sea heat content and its variability.

[20] As these mechanisms in turn are governed by atmospheric, cryospheric and hydrographic variability, a variety of cross-connections has to be analyzed. Furthermore, the atmospheric fluxes needs to be divided into solar and non-solar components (Figure 5).

[21] In the following, the relative importance and time scales of strongest influence from oceanic transport versus atmospheric fluxes will be assessed accordingly.

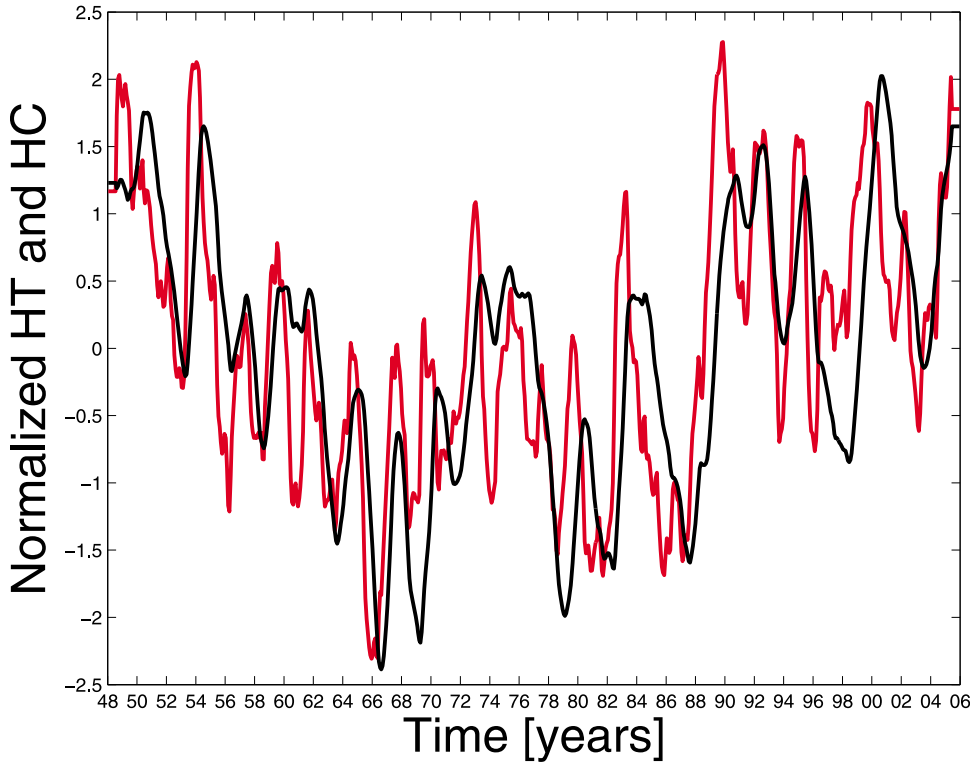

Figure 3. Normalized time series for the heat transport (HT) through the BSO into the Barents Sea (red) and the heat content (HC) in the Barents Sea (black). A 12 months running mean filter is used on monthly time series.

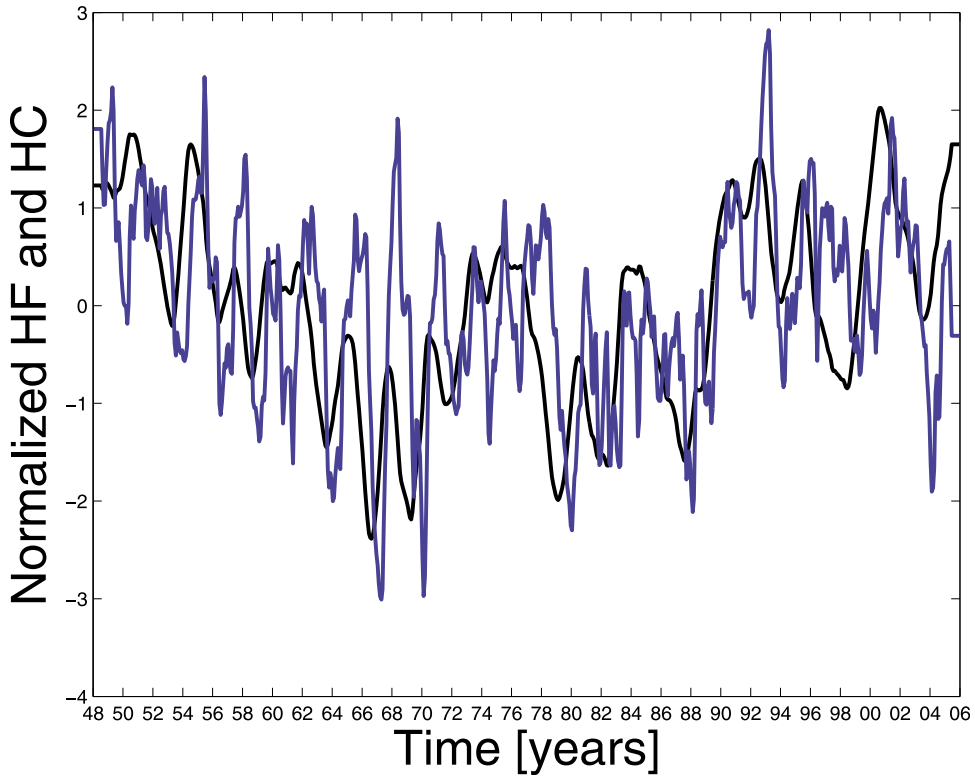

Figure 4. Normalized time series for the heat content in the Barents Sea (black) and the upward heat flux (HF) to the atmosphere (blue). A 12 months running mean filter is used on monthly time series.

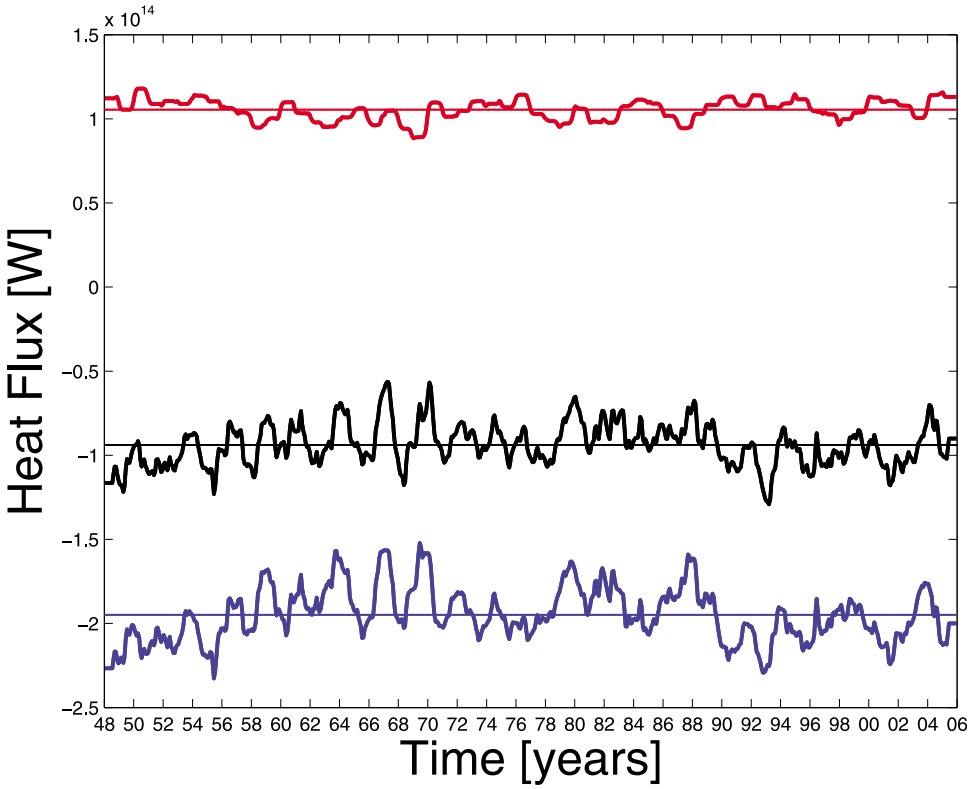

Figure 5. Time series for the solar (red), non-solar (blue), and net heat flux (black) into the Barents Sea. All fluxes are in W and defined positive downward, and a 12 months running mean filter is used on monthly time series.

4.3. Mechanisms Behind the Heat Content Variability

[22] Based on the apparent lags in Figures 3 and 4, and on the amplitudes and mean values of the components in Figure 5, our hypothesis is: Changes in the solar heat flux and the heat transport through the BSO are the main causes for Barents Sea heat content variability. Thereafter, this heat content variability leads to corresponding changes in the non-solar heat flux.

[23] The solar time series accounts for incoming solar short wave radiation (output from the atmospheric reanalysis) adjusted for albedo (model), cloud cover (reanalysis) and ice fraction (model), while the non-solar time series account for long wave radiation, latent and sensible heat fluxes (model) (Figure 5). From the model used here, only the two time series for solar and non-solar heat fluxes are available. The individual effects of the non-solar components longwave radiation, sensible heat and latent heat on the Barents Sea climate are therefore not accessible. It is possible that some of these components separately influence the heat content in a different way than their combination. The fact that the components for the heat fluxes include effects of cloud cover and ice fraction also complicates the understanding of their relative importance for the variability, but hypotheses for these processes can still be made for later studies.

[24] For the above hypothesis to be valid, there must be a significant correlation with a certain lag between the successive time series. The chain of events can be checked by performing correlation analyzes where all relevant time series are included. The resulting correlations and lags are listed in Table 1, and all numbers are significant according to the method by *Chelton* [1983].

[25] The largest correlation is found for heat content lagging the solar influx by 2 months. Then follows the correlation for heat content lagging the BSO heat transport by 1 month. The third strongest correlation is found for heat content leading the non-solar heat flux with 1 month. These relations are all in line with our hypothesis.

[26] With respect to units, a more consistent way to compare time series would be to correlate the heat transport and fluxes with the time derivative of Barents Sea heat content (rate of change). The results of such correlations are shown in Figure 6, and give as expected high correlations, but at no time lags. This means that there is an immediate

Table 1. Peak Correlations and Lags Between Barents Sea Heat Content and Potential External Forcing Factors, Based on Deseasoned and Detrended Monthly Time Series[a]

	Heat Content	Heat Content West	Heat Content East
Heat Flux	−0.29 at −1	−0.20 at −1	−0.37 at −1
Heat Flux Solar	0.53 at 2	0.37 at 1	0.58 at 2
Heat Flux Non-Solar	−0.42 at −1	−0.31 at −1	−0.51 at −1
Heat Transport	0.48 at 1	0.52 at 1	0.42 at 8

[a]Heat content, heat content west, and heat content east represent the entire Barents Sea, western region, and eastern region, respectively. Lags are defined as positive when heat content lags the forcing factors. The reference direction for all heat fluxes is downward.

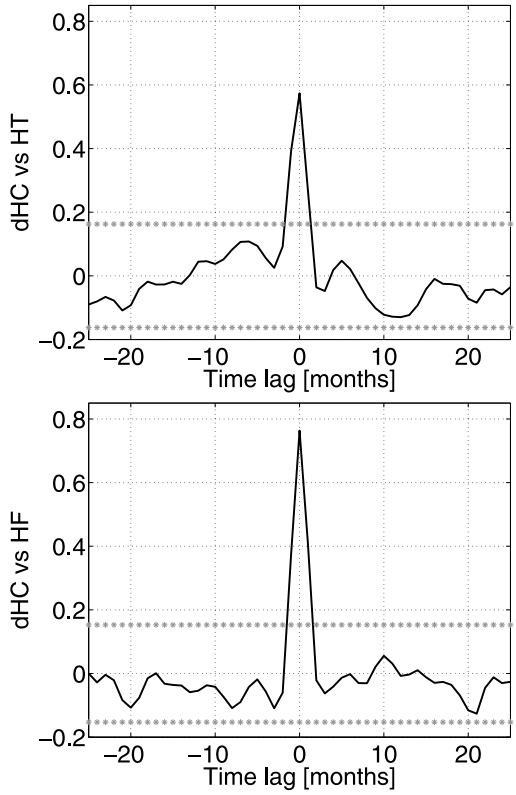

Figure 6. Correlation at lags between the rate of change in heat content and the (top) heat transport through the BSO and (bottom) heat flux to the atmosphere. The significance levels are indicated by horizonal lines. Sign conventions as defined in Table 1.

response in the rate of change in heat content to variability in heat transport and heat flux.

[27] On the other hand, it is the actual heat content over the whole Barents Sea that is important for the ecosystem. To predict this, we exploit that there is a lag between the point of time when the warm waters enter the BSO and when these waters are advected and spread into the Barents Sea and thereby influence the heat content. Likewise for the heat fluxes at the surface and the vertical mixing of heat.

[28] To assess the relative importance of heat transport and heat flux, both close to the inflow and in the farther reaches of the Barents Sea, our study area is divided into a western and an eastern region as shown in Figure 1. From Table 1 it can be concluded that the solar heat flux has strongest correlation to the heat content in the eastern region where the ice cover variability is relatively large, even though the ice fraction there is twice as large as in the western region. In the model, solar radiation is attenuated by the ice concentration before reaching the top layer of the ocean, and variations in ice concentration will therefore strongly influence the solar radiation variability. In this way, the ice cover can be interpreted as a switch for the solar heat flux. In the western region, the ice edge is more or less locked by the topographically steered Polar Front along the bottom slope from Bear Island to Central Bank, and the heat transport dominates the heat content variability there. The greater correlation with heat transport in this area can also be explained in terms of the short distance to the BSO.

[29] Extending the analysis to include the ice fraction of the Barents Sea, Table 2 shows that there is a relatively large and immediate response of the ice fraction on the heat content, or vice versa. Like the heat content, the ice fraction lags the heat transport and lead the non-solar heat flux, supporting the strong relation between heat content and ice cover. Figure 7 summarizes how heat content is influenced by heat transport, solar heat flux and ice fraction with various lags and correlations, and how it to a lesser extent affects the non-solar and net heat fluxes.

4.4. Lags and Filtering

[30] The lags found (Table 1) are small compared to those apparent in Figure 3, due to the use of a 12 month running mean filter to avoid noise in the plotted time series. A comparison of correlation analysis using monthly versus annual time series of heat content and heat transport is shown in Figure 8: The monthly time series yield significant correlations at lags from 1 to 13 months while the corresponding result from the annual series is 0 and 1 year. Concurrently, using a 12 month running mean filter on the monthly time series yields a peak at 7 months (not shown). Using heat content and solar heat flux in the comparison shows the same effect of resolution and filtering (Figure 9): The annual series yield a lag at 0 years, while the monthly, as well as filtered (not shown), series yield a broader band of significant correlations around a peak at 2 months lag. The physical conclusion from these revealed lags at different resolution is that only ocean heat transport has a potential for delivering predictability of the Barents Sea heat content in the range of 1 year ahead.

4.5. Common Forcing

[31] On interannual to decadal time scales, all time series related to the Barents Sea climate in Figures 3–5 seem to have about the same variability, which may be due to a common forcing mechanism. Several studies on ocean variability emphasize the importance of the North Atlantic Oscillation (NAO) [*Sutton and Allen*, 1997; *Eden and Willebrand*, 2000], one of the most important drivers of climate fluctuations in the North Atlantic and surrounding humid climates. *Nilsen et al.* [2003] and *Mauritzen et al.* [2006] used MICOM to show a relation between NAO and the inflow of Atlantic waters, both with respect to volume transport and hydrographic variability in the Norwegian Atlantic Current (NwAC). There are therefore reasons to believe that this relation is valid to some extent also

Table 2. Peak Correlations and Lags Between Barents Sea Ice Fraction and Potential External Forcing Factors, Based on Deseasoned and Detrended Monthly Time Series[a]

	Ice Fraction
Heat Content	−0.78 at −1,0
Heat Flux	0.21 at −7
Heat Flux Solar	−0.60 at 0
Heat Flux Non-Solar	0.40 at −1
Heat Transport	−0.46 at 1

[a]Lags are defined as positive when ice fraction lags the forcing factors. The reference direction for all heat fluxes is downward.

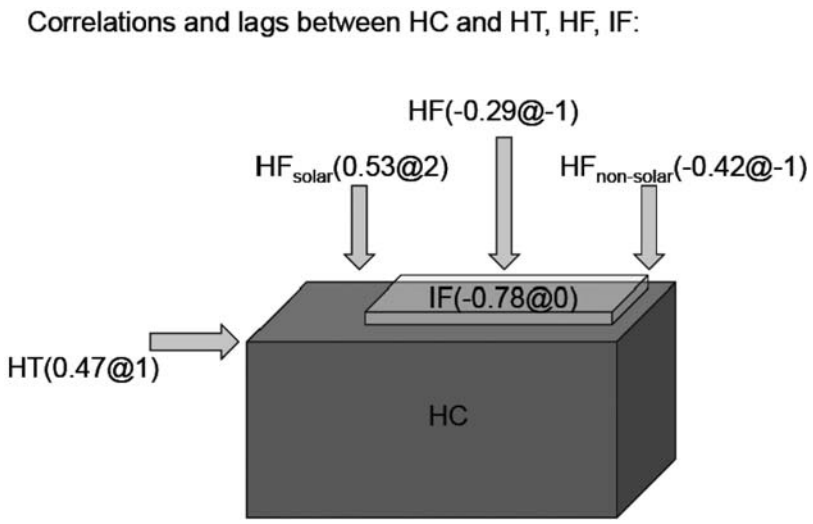

Figure 7. Correlation at lags between the heat content and the main contributors to the heat content variability. Sign conventions as defined in Table 1.

for the BSO-inflow, as it is a bifurcated part of the NwAC, following topography into the Barents Sea. *Kärcher et al.* [2003] used another numerical model to show an intensified eastward BSO volume transport associated with a wind stress pattern having strong cyclonicity over the central Nordic Seas, while *Ingvaldsen et al.* [2004] used reconstructed velocity fields to reveal the importance of the Icelandic Low and its associated trough stretching across the Nordic Seas towards the Barents Sea, on the BSO inflow.

[32] Figure 10 shows results from a regression and correlation analysis between the modeled BSO annual volume transports and the NCEP/NCAR [*Kalnay et al.*, 1996]

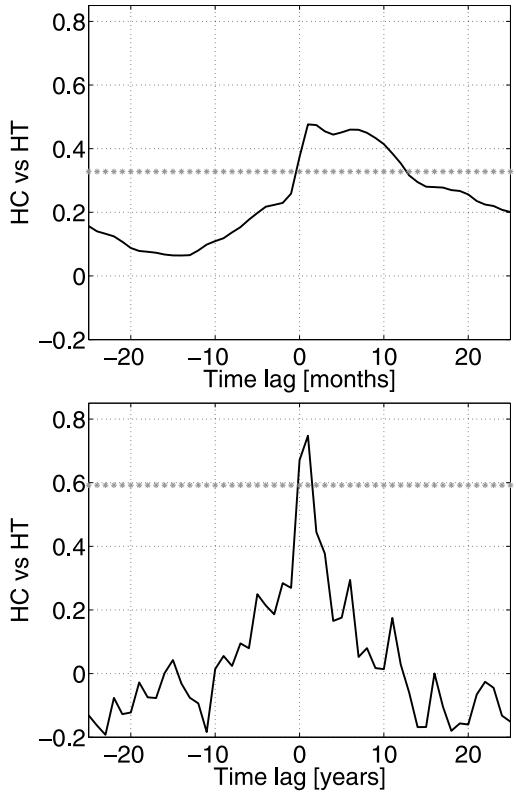

Figure 8. Correlation at lags between the heat content and heat transport using (top) monthly and (bottom) annual time series. The significance levels are indicated by horizonal lines. Sign conventions as defined in Table 1.

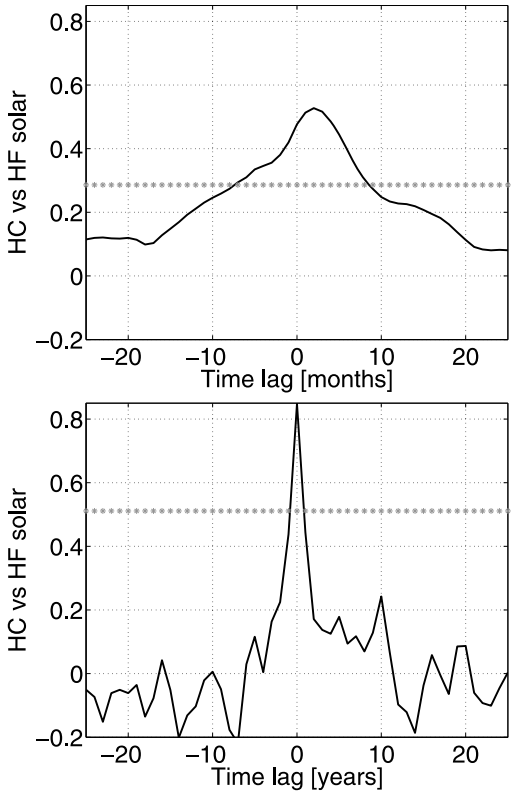

Figure 9. Correlation at lags between the heat content and solar heat flux using (top) monthly and (bottom) annual time series. The significance levels are indicated by horizonal lines. Sign conventions as defined in Table 1.

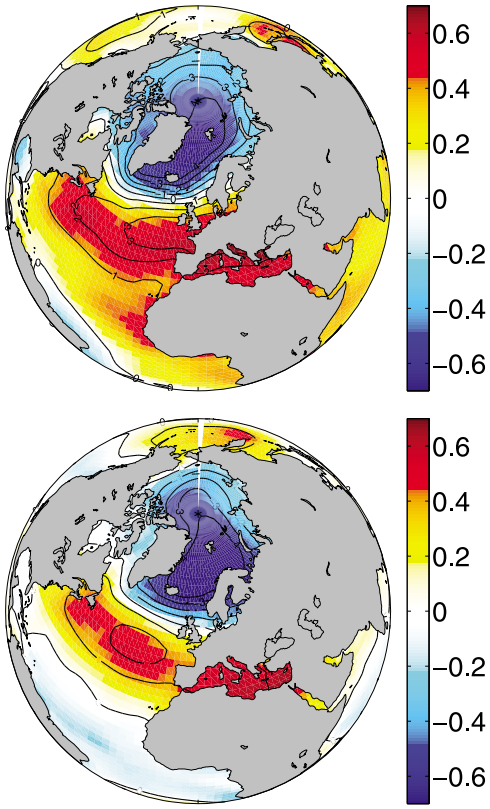

Figure 10. Regression (contours) and correlation (colors) between the modeled BSO volume transports and SLP for the two sub-periods 1948–1977 and 1978–2006. A 12 months running mean filter is used. The regression relates SLP-anomalies in hPa to volume transport anomalies through the BSO of 1 Sv.

reanalyzed global atmospheric sea level pressure (SLP) and reveals positive transport anomalies to be associated with high pressure over the Azores and low pressure over the Nordic Seas. The latter moves slightly eastward during the integration period, from a position with center in the Greenland Sea to one with center very close to the BSO. The pattern is similar to the observed NAO, which allows a connection to the NAO also for the BSO. The position of the northern regression and correlation minimum, especially in the 1978–2006 period, favors control of NAO on the Atlantic inflow to the Barents Sea. It can be seen that an interannual change of 1 Sv in the BSO inflow corresponds to a change in the atmospheric pressure of approximately 4 hPa. The modeled transports have interannual variations of about 0.8 Sv, corresponding to an atmospheric pressure change of about 3 hPa.

[33] Similarly, the heat transport in the BSO (Figure 11a), solar heat flux (Figure 11b), and heat content (Figure 11c) are also correlated to SLP. All three show a similar NAO pattern to that seen in Figure 10, and the regressions show that the variability of the heat transport and the solar heat flux are about equally influenced by the SLP. The amplitude of the interannual variations are about 20 TW for both time series (not shown) which corresponds to variations in the annual averaged low pressure in the Nordic Seas of about 3 hPa.

[34] The non-solar heat flux does not correlate to NAO (not shown), and as a result, nor does the net heat flux, unless the series are filtered to represent decadal variability (Figure 11d). This indicates a relatively immediate response of heat transport and solar heat flux to NAO, while the non-solar heat flux is influenced by other sources of variability on interannual time scale.

4.6. Long-Term Changes

[35] During the integration period of this study, an eastward shift in the northern center of action of the NAO has been observed [*Hilmer and Jung*, 2000].

[36] The shifted NAO has been shown to have strong influence on the flow variability of the boundary currents in the Nordic Seas, since it dominates the variability of both the North Atlantic westerlies and the northerlies along the east coast of Greenland [*Nilsen et al.*, 2003].

[37] This also seems to be the case for the Barents Sea inflow (Figure 10). Temporal changes in the relative influences of heat transport and heat flux on heat content variability, are assessed by performing correlation analysis on two subperiods, 1948–1977 and 1978–2006 (Table 3). The two subperiods display a strengthening of the correlation between NAO and the heat transport trough the BSO (Table 3). The effects of a shifted NAO on the heat content and the other forcing factors is negligible compared to this.

5. Discussion

[38] Due to the ample supply of Atlantic waters, the intense ocean-atmosphere heat exchange, and the formation of ice, the Barents Sea is a key region in the North Atlantic and Arctic Ocean climate system [*Simonsen and Haugan*, 1996]. Changes in the Barents Sea climate has already been linked to anomalous heat and volume transport in Atlantic waters from the Nordic Seas [*Furevik*, 2001], based on the use of 16 years of data from five regular sections across the flow of Atlantic waters in the Nordic Seas. Based on common knowledge about Atlantic Water inflow and heat loss to the atmosphere, it is clear that the average non-solar heat flux must compensate for more than the average solar heat flux in order to conserve the heat budget. Here in this study we focus on the relative importance of advective heat transports and ocean-atmosphere heat fluxes and their roles in the Barents Sea climate variability. Specific knowledge about the processes that are important for the climate variability, and their corresponding correlation and time lag, can provide information about where and when to take observations, and to what extent these explain the heat content some time in advance.

[39] The hypothesis in this study on climate variability is based on inspection of modeled time series for heat transport, heat content and heat flux. It suggests that (1) transport of heat through the BSO and atmosphere-ocean solar heat flux control the heat content variability with some time lag and (2) heat content anomalies lead to corresponding changes in the non-solar heat fluxes. Systematic correlations between the involved time series support these statements, and provide numbers for correlations and lags on different time scales indicating their relative importance. Very similar

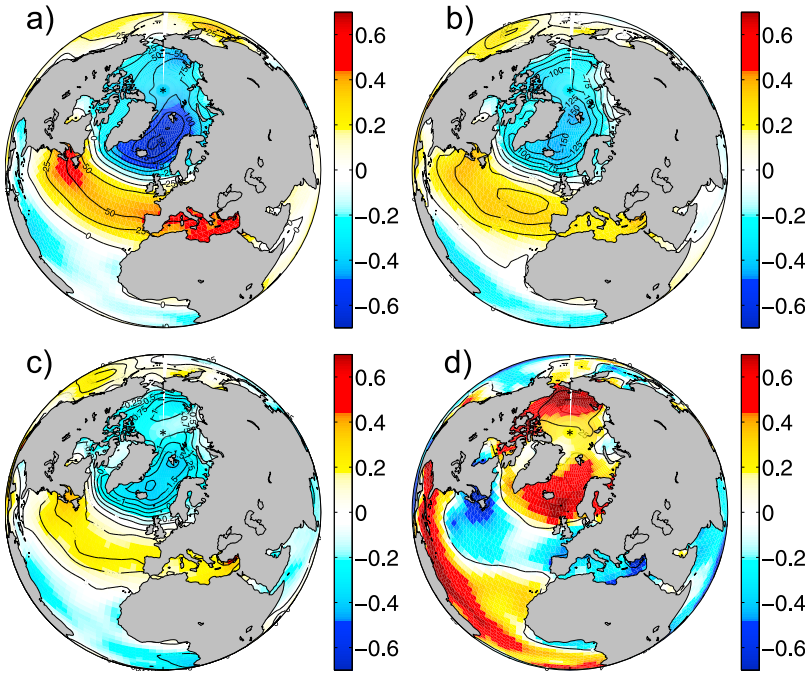

Figure 11. Regression (contours) and correlation (colors) between SLP (1948–2006) and the (a) modeled BSO heat transports, (b) solar heat flux into the ocean, (c) heat content, and (d) non-solar heat flux into the ocean. A 12 months running mean filter is used for the BSO heat transports, the solar heat flux, and the heat content, while a 10 years running mean is used for the non-solar heat. The regression relates SLP-anomalies in hPa to heat transport and -flux anomalies of 1 PW, and to heat content anomalies of 1 ZJ ($Z = 10^{21}$).

correlation-lag relationship between heat transport and heat content was found by M. Årthun and C. Schrum (Ocean surface heat flux variability in the Barents Sea, submitted to *Journal of Marine Systems*, 2009), using the regional coupled ice- ocean model HAMSOM.

[40] The variability and mean value of the non-solar heat flux is considerably larger than the solar heat flux, and the non-solar component dominates the net heat flux. This is probably the reason that the net heat flux lags the heat content even if the solar heat flux leads the heat content. And even though the solar heat flux shows strongest correlation to the heat content, the variable best suited for prediction of the Barents Sea climate variability on annual time scale is the heat transport, which on average leads the heat content by several months. The heat content for the entire Barents Sea is an important component in this study as it physically accounts for the delay in the advection of heat from the BSO. The heat content reflects the average temperature, and the ice fraction is therefore strongly correlated to the heat content with no delay.

[41] As pointed out in Section 4.5, all time series related to the Barents Sea climate display similar variability, at least on decadal time scale. Furthermore, almost all correlations of the different time series with SLP reveal strong relations to NAO, a mode of atmospheric variability with strong influence on the ocean variability [*Hurrell*, 1995]. Even though the non-solar radiation is much stronger than the solar heat flux and is significantly correlated to the heat content, its time series regressed against SLP does not correspond to the NAO pattern. With the exception of the non-solar heat flux, all time series herein considered to be important for the Barents Sea climate variability, correlate to a pattern similar to the NAO, both on interannual and

Table 3. Peak Correlations and Lags Between Annually Averaged and Detrended Time Series for the Periods 1948–1977 and 1978–2006[a]

	Heat Content	Heat Flux	Heat Flux Solar	Heat Flux Non-Solar	Heat Transport
Heat Content					
1948–1977	-	-	0.81 at 0	−0.66 at 0	0.69 at 1
1978–2006	-	-	0.89 at 0	−0.71 at 0	0.66 at 1
Ice Fraction					
1948–1977	−0.87 at 0	0.51 at −1	−0.90 at 0	0.60 at −1	-
1978–2006	−0.89 at 0	-	−0.90 at 0	-	-
NAO					
1948–1977	0.52 at 1	-	-	-	0.52 at 0
1978–2006	0.45 at 1	-	-	-	0.73 at 0

[a]Only significant correlations are shown. Sign conventions as defined in Tables 1 and 2.

decadal time scales. The physical explanation for these relations might be as follows:

[42] 1. Variations in NAO cause variations in the westerlies, which again are responsible for changes in atmospheric, and thereby oceanic transports. As a result of this, there is a positive correlation between NAO and BSO heat transport. The larger scale version of NAO, the Arctic Oscillation (AO), has also been shown to correlate with heat transports through the BSO (Årthun and Schrum, submitted manuscript, 2009).

[43] 2. Anomalies in heat transport, and subsequently in heat content, correspond to anomalies in ice cover with no lag to heat content. As the solar heat flux is a function of ice fraction in the model there is a positive correlation between NAO and solar heat flux.

[44] 3. Northward-moving cyclones traveling into the Arctic over East Siberia are found to influence winds and ice extent over the Barents Sea strongly [*Sorteberg and Kvingedal*, 2006]. The corresponding winds influence the non-solar heat flux (in terms of sensible, latent and long-wave radiation) on interannual time scales or shorter. The NAO signal in the non-solar heat flux might therefore disappear at shorter time scales when this heat flux is more influenced by cyclones from e. g. East Siberia. On longer time scales, successive years of high or low NAO might lead to greater anomalies in the heat content and there is a correlation to a NAO-like pattern on decadal time scales. A similar mechanism for salinity anomalies is proposed by *Sundby and Drinkwater* [2007]: The varying volume fluxes in and out of the Arctic Basin is the causal mechanism behind the anomaly signals, the NAO partly influences the flux, and periods of large decadal-scale amplitudes of NAO coincide with periods of large decadal-scale oscillations in the marine climate.

[45] The above reasoning and the numbers for the correlations given in Tables 1–3 indicate that the processes suggested to be important for the Barents Sea climate variability act different depending on region and time scale, and that there is a common forcing mechanism behind.

[46] With regard to trends, there is a significant increase in correlation between NAO and the heat transport through the BSO due to the eastward shift in NAO. However, there is a decrease in the correlation between the heat content and NAO in this period. The explanation might be the increased correlation to the solar and non-solar heat fluxes.

[47] To summarize, solar heat flux has greater correlation to heat content, but heat transport has greater potential for predictability. Heat transport and solar heat flux are equally regressed to the SLP, but the correlations are different. The respective correlations for the annual time series of solar heat flux and heat transport with respect to heat content are 0.85 and 0.75, which explain 72% and 56% of the variability.

[48] The importance of solar heat flux and heat transport to the Barents Sea climate variability as shown in this study does not exclude any influence of individual non-solar heat flux components, but it is doubtful that such an influence will exceed the period of predictability related to the heat transport through the BSO, since the vertical heat exchange between the ocean and atmosphere is in general faster than horizontal advection of heat. The study here has revealed some of the dominating mechanisms behind the Barents Sea climate variability and their potential in the forecasting of regional climate.

6. Summary and Conclusions

[49] This model study on the regional climate variability in the Barents Sea reveals: (1) there is a good fit between the modeled and observed temperatures in the Kola Section (r = 0.89); (2) heat transport through BSO, solar heat flux, and ice fraction are all important to climate variability in the Barents Sea; (3) there is a potential to forecast heat content in the Barents Sea based on annual averages of heat transport through the BSO 1 year ahead; (4) heat transports, solar heat fluxes, and heat content are all correlated to NAO; (5) non-solar heat flux is correlated to a NAO-like pattern on decadal time scales, which means that heat loss to the atmosphere is correlated to NAO; (6) and there is an increased correlation between heat transport through the BSO and NAO over the last 30 years.

[50] **Acknowledgments.** This work was supported by the Norwegian Research Council projects NESSAS, NorClim, POCAHONTAS, and BIAC, and by the Norwegian Supercomputer Committee through a grant of computing time. Valuable discussions and comments in the "Barents Sea group" at GFI/BCCR/IMR/NERSC is much appreciated. This is publication A 285 from the Bjerknes Centre for Climate Research.

References

Bentsen, M. (2002), Modelling ocean climate variability of the North Atlantic and the Nordic Seas, Ph.D. thesis, Nansen Environ. and Remote Sens. Cent., Bergen, Norway.

Bentsen, M., and H. Drange (2000), Parameterizing surface fluxes in ocean models using the NCEP/NCAR reanalysis data, *RegClim Gen. Tech. Rep. 4*, Norw. Inst. for Air Res., Kjeller, Norway.

Bentsen, M., H. Drange, T. Furevik, and T. Zhou (2004), Simulated variability of the Atlantic meridional overturning circulation, *Clim. Dyn.*, *22*, 701–720.

Berliand, M., and T. Berliand (1952), Determining the net long-wave radiation of the earth with consideration of the effect of cloudiness, *Izv. Akad. Nauk. SSSR Ser. Geofiz.*, *1*, 64–78.

Bleck, R., C. Rooth, D. Hu, and L. T. Smith (1992), Salinity-driven thermocline transients in a wind- and thermohaline-forced isopycnic coordinate model of the North Atlantic, *J. Phys. Oceanogr.*, *22*, 1486–1505.

Chelton, D. B. (1983), Effects of sampling errors in statistical estimation, *Deep Sea Res. Part A*, *30*, 1083–1103.

Drange, H., and K. Simonsen (1996), Formulation of air-sea fluxes in the ESOP2 version of MICOM, *Rep. 125*, Nansen Environ. and Remote Sens. Cent., Bergen, Norway.

Drange, H., R. Gerdes, Y. Gao, M. Kärcher, F. Kauker, and M. Bentsen (2005), Ocean general circulation modelling of the Nordic Seas, in *The Nordic Seas: An Integrated Perspective*, edited by H. Drange et al., pp. 199–219, AGU, Washington, D. C.

Drinkwater, K. F., F. Mueter, K. D. Friedland, M. Taylor, G. L. Hunt Jr., J. Hare, and W. Melle (2009), Recent climate forcing and physical oceanographic changes in Northern Hemisphere regions: A review and comparison of four marine ecosystems, *Prog. Oceanog.*, *73*, 190–202.

Dukowicz, J., and J. Baumgardner (2000), Incremental remapping as a transport/advection algorithm, *J. Comput. Phys.*, *160*, 318–335.

Eden, C., and J. Willebrand (2000), Mechanism of interannual to decadal variability in the North Atlantic Ocean, *J. Clim.*, *14*, 2266–2280.

Eldevik, T., F. Straneo, A. B. Sandø, and T. Furevik (2005), Pathways and export of Greenland Sea Water, in *The Nordic Seas: An Integrated Perspective*, edited by H. Drange et al., pp. 89–103, AGU, Washington D. C.

Fairall, C. W., E. F. Bradley, D. P. Rogers, J. B. Edson, and G. S. Young (1996), Bulk parameterization of air-sea fluxes for tropical ocean-atmosphere response experiment, *J. Geophys. Res.*, *101*, 3747–3764.

Furevik, T. (2001), Annual and interannual variability of Atlantic Water temperatures in the Norwegian and Barents Seas: 1980–1996, *Deep Sea Res. Part I*, *48*, 383–404.

Furevik, T., M. Bentsen, H. Drange, I. K. T. Kindem, N. G. Kvamstø, and A. Sorteberg (2003), Description and validation of the Bergen Climate Model: ARPEGE coupled with MICOM, *Clim. Dyn.*, *21*, 27–51.

Gammelsrød, T., Ø. Leikvin, V. Lien, W. P. Budgell, H. Loeng, and W. Maslowski (2009), Mass and heat transports in the NE Barents Sea: Observations and models, *J. Mar. Syst.*, *75*, 56–69.

Gao, Y., H. Drange, M. Bentsen, and O. M. Johannessen (2004), Simulating transport of non-Chernobyl 137Cs and 90Sr in the North Atlantic-Arctic region, *J. Environ. Radioact.*, *71*, 1–16.

Harder, M. (1996), Dynamik, rauhigkeit und alter des meereises in der Arktis, Ph.D. thesis, Alfred Wegener Inst. für Polar- und Meeresforsch., Bremerhaven, Germany.

Harms, I. H., C. Schrum, and K. Hatten (2005), Numerical sensitivity studies on the variability of climate-relevant processes in the Barents Sea, *J. Geophys. Res.*, *110*, C06002, doi:10.1029/2004JC002559.

Hátún, H., A. B. Sandø, H. Drange, and M. Bentsen (2005a), Seasonal to decadal temperature variations in the Faroe-Shetland inflow waters, in *The Nordic Seas: An Integrated Perspective*, edited by H. Drange et al., pp. 239–238, AGU, Washington D. C.

Hátún, H., A. B. Sandø, H. Drange, B. Hansen, and H. Valdimarsson (2005b), Influence of the Atlantic Subpolar Gyre on the thermohaline circulation, *Science*, *309*, 1841–1844.

Hibler, W. D., III (1979), A dynamic thermodynamic sea ice model, *J. Phys. Oceanogr.*, *9*, 815–846.

Hilmer, M., and T. Jung (2000), Evidence for a recent change in the link between the North Atlantic Oscillation and Arctic sea ice export, *Geophys. Res. Lett.*, *27*, 989–992.

Hughes, S. L., N. P. Holliday, E. Colbourne, V. Ozhigin, H. Valdimarsson, S. Østerhus, and K. Wiltshire (2009), Comparison of in situ time-series of temperature with gridded sea surface temperature datasets in the North Atlantic, *ICES J. Mar. Sci.*, *66*, 1467–1479.

Hurrell, J. W. (1995), Decadal trends in the North Atlantic oscillation: Regional temperatures and precipitation, *Science*, *269*, 676–679.

Ingvaldsen, R. B., L. Asplin, and H. Loeng (2002), The seasonal cycle in the Atlantic transport to the Barents Sea during the years 1997–2001, *Cont. Shelf Res.*, *24*, 1015–1032.

Ingvaldsen, R. B., L. Asplin, and H. Loeng (2004), Velocity field of the western entrance to the Barents Sea, *J. Geoph. Res.*, *109*, 1–12.

Kalnay, E., et al. (1996), The NCEP/NCAR 40-year reanalysis project, *Bull. Am. Meteorol. Soc.*, *77*, 437–471.

Kärcher, M. J., R. Gerdes, F. Kauker, and C. Koberle (2003), Arctic warming: Evolution and spreading of the 1990s warm event in the Nordic Seas and the Arctic Ocean, *J. Geophys. Res.*, *108*(C2), 3034, doi:10.1029/2001JC001265.

Ledwell, J. R., A. J. Watson, and C. S. Law (1993), Evidence for slow mixing across the pycnocline from open-ocean tracer-release experiment, *Nature*, *364*, 701–703.

Levitus, S., and T. P. Boyer (1994), *World Ocean Atlas 1994*, vol. 4, *Temperature, NOAA Atlas NESDIS*, vol. 4, 129 pp., NOAA, Silver Spring, Md.

Levitus, S., R. Burgett, and T. P. Boyer (1994), *World Ocean Atlas 1994*, vol. 3, *Salinity, NOAA Atlas NESDIS*, vol. 3, 111 pp., NOAA, Silver Spring, Md.

Mauritzen, C., S. S. Hjøllo, and A. B. Sandø (2006), Passive tracers and active dynamics—A model study of hydrography and circulation in the northern North Atlantic, *J. Geophys. Res.*, *111*, C08014, doi:10.1029/2005JC003252.

Nilsen, J. E. Ø., Y. Gao, H. Drange, T. Furevik, and M. Bentsen (2003), Simulated North Atlantic-Nordic Seas water mass exchanges in an isopycnic coordiante OGCM, *Geophys. Res. Lett.*, *30*(10), 1536, doi:10.1029/2002GL016597.

Orre, S., Y. Gao, H. Drange, and J. E. Ø. Nilsen (2007), A reassessment of the dispersion properties of 99Tc in the North and Norwegian Seas, *J. Mar. Syst.*, *30*, 24–38.

Sakshaug, E., A. Bjørge, B. Gulliksen, H. Loeng, and F. Mehlum (1994), Structure, biomass distribution, and energetics of the pelagic ecosystem in the Barents Sea: A synopsis, *Polar Biol.*, *14*, 405–411.

Simonsen, K., and P. M. Haugan (1996), Heat budgets of the Arctic Mediterranean and sea surface flux parameterizations of the Nordic Seas, *J. Geophys. Res.*, *101*, 6553–6576.

Skagseth, Ø., T. Furevik, R. Ingvaldsen, H. Loeng, K. A. Mork, K. A. Orvik, and V. Ozhigin (2008), Volume and heat transports to the Arctic Ocean via the Norwegian and Barents Seas, in *Arctic-Subarctic Ocean Fluxes (ASOF)*, edited by R. R. Dickson, J. Meincke, and P. Rhines, pp. 1–29, Springer, New York.

Smedsrud, L. H., R. Ingvaldsen, J. E. Ø. Nilsen, and Ø. Skagseth (2010), Heat in the Barents Sea: Transport, storage, and surface fluxes, *Ocean Sci.*, *6*, 219–234.

Smith, S. D. C. W. F., G. L. Geemaert, and L. Hasse (1996), Air-sea fluxes: 25 years of progress, *Boundary Layer Meteorol.*, *78*, 247–290.

Sorteberg, A., and B. Kvingedal (2006), Atmospheric forcing in the Barents Sea winter sea ice extent, *J. Clim.*, *19*, 4772–4784.

Sundby, S., and K. Drinkwater (2007), On the mechanism behind salinity anomaly signals of the northern North Atlantic, *Prog. Oceanogr*, *73*, 190–202.

Sutton, R. T., and M. R. Allen (1997), Decadal predictability of North Atlantic sea surface temperature and climate, *Nature*, *388*, 563–567.

Y. Gao and J. E. Ø. Nilsen, Nansen Environmental and Remote Sensing Center, Thormøhlensgt. 47, N-5006 Bergen, Norway.

K. Lohmann, Max Planck Institute for Meteorology, Bundesstr. 53, D-20146 Hamburg, Germany.

A. B. Sandø, Institute of Marine Research, PO Box 1870, Nordnes, N-5817 Bergen, Norway. (anne.britt.sando@imr.no)